Dependence of the direct energy gap of GaAs on hydrostatic pressure

Benjamin Welber
IBM Thomas J. Watson Research Center, Yorktown Heights, New York 10598

Manuel Cardona
Max-Planck-Institut für Festkörperforschung, Stuttgart, Federal Republic of Germany and IBM Thomas J. Watson Research Center, Yorktown Heights, New York 10598*

C. K. Kim† and Sergio Rodriguez‡
Max-Planck-Institut für Festköperforschung, Stuttgart, Federal Republic of Germany

(Received 9 July 1975)

A measurement of the dependence of the direct energy gap of GaAs on hydrostatic pressure is reported. Pressures up to 180 kbar were applied with a diamond anvil cell and measured using the ruby luminescence technique. At 180 kbar the material experiences a transition to a phase which is opaque in the visible region of the electromagnetic spectrum. The energy gap $E_0(\text{eV}) = 1.45 + 1.26 \times 10^{-2}P - 3.77 \times 10^{-5}P^2$ (P is the pressure in kbar) exhibits a strong nonlinear dependence on P. The dependence of E_0 on the lattice parameter is more nearly linear but still sublinear in the relative change of lattice constant. A theoretical study of this nonlinearity is carried out using the method of the pseudopotential. We find that the observed sublinearity of E_0 on the lattice parameter can be accounted for by supposing that the core radius varies quadratically with the relative change of this quantity. Finally, our results are compared with those of the empirical dielectric theory.

I. INTRODUCTION

Measurements of the dependence of energy gaps of semiconductors on hydrostatic pressure have been valuable tools for band-structure studies, especially for materials of the germanium–zinc-blende family.[1] It was recognized[2] early that for a given family of materials equivalent energy-band extrema had very similar pressure coefficients but that these coefficients varied widely among nonequivalent extrema. This fact was used to identify the symmetries of the lowest absorption edges of the germanium–zinc-blende type materials. Among these semiconductors, GaAs occupies a prominent position because of its technological interest. The fundamental direct absorption edge of this material, labeled E_0, was studied by Sturge[3] at several temperatures and shown to be strongly affected by excitonic interactions. E_0 corresponds to transitions between the Γ_{15} top of the valence band and the lowest conduction-band minimum Γ_1, both extrema being located at the center of the Brillouin zone. A large number of studies of the hydrostatic-pressure coefficient of this edge have been performed since the early work of Paul and Warschauer.[4] Their results are displayed in Table I. These studies can be classified into three types according to the pressure techniques used.

(i) The first is pure hydrostatic pressure using relatively large samples and pressure vessels (available volume ~1 cm²), a pressure-transmitting fluid, and usually sapphire windows.[4,5] The upper limit of the pressures reached with this technique is about 10 kbar.

(ii) Second, we have quasihydrostatic pressure, using a plastic solid (NaCl) as a transmitting fluid. In this technique, pioneered by Drickamer and coworkers,[6] pressures up to 150 kbar are reached. The results obtained, however, cannot be compared directly with those of other methods because the pressure calibrations used in such optical cells are now known to be (10–15)% too high, and because only thick samples can be measured. The pressure dependence of the direct gap of GaAs obtained by this method[7] falls short of that found with any other technique, as can be seen from Table I. The discrepancy, however, may be mainly due to the errors in the pressure scale.

(iii) Lastly, we have application of a uniaxial compression to an elongated prism of the material. This compression has pure hydrostatic and pure shear components. By judiciously combining optical measurements for polarizations parallel to and perpendicular to the stress, the effect of the hydrostatic component can be extracted.[8] Particular care must be taken of the fact that, owing to coupling of the spin-orbit-split valence bands by the *uniaxial* stress the shifts of the gaps observed are somewhat nonlinear.[8]

While the three methods given above refer to the pressure technique used, different procedures are employed in the determination of the energy gap as a function of pressure. The simplest method[4,7]

consists in measuring the transmission of samples thin enough (10 μm) so that they permit the observation of coefficients in the direct exciton region ($\sim 10^4$ cm^{-1}). Measurements with thicker samples[7] lead to results which are not characteristic of the direct absorption edge. Very accurate measurements can be performed by using GaAs laser diodes operated below threshold in the spontaneous-emission mode[9,10] or with more conventional luminescence techniques.[11] Excellent accuracy can also be obtained with any of several reflection-modulation techniques such as piezoreflectance,[12] electroreflectance,[8] and wavelength modulation.[13] Electrical methods, such as Hall-effect measurements[14] and I-V measurements in tunnel junctions[15] as functions of pressure have also been used to determine the pressure coefficient of the E_0 gap.

The linear pressure coefficient of the E_0 gap of GaAs has been calculated by several methods such as the orthogonalized-plane-wave (OPW) work of Collins *et al.*,[16] the pseudopotential work of Melz[17] and of Neumann *et al.*,[18] the empirical dielectric method[19] (see Table I), and the relativistic OPW work of Melz and Ortenburger.[20]

Recent developments in the field of high-pressure technology[21] enable one to perform measurements with pure hydrostatic pressures up to at least 120 kbar with diamond anvil cells. The pressure is determined from the shift in the fluorescence lines of a piece of ruby placed in the microscopic cell.

TABLE I. Linear pressure coefficients of the E_0 gap of GaAs found by other authors. Since the experimental determinations in this table neglected the sublinearity in the pressure dependence of E_0, the coefficients are smaller than that found in the present work (12.6± 0.1, in units of 10^6 eV/bar).

Experiment: uniaxial stress	Experiment: hydrostatic stress	Theory
11.7± 0.5 [a]	11.3± 0.2 [e]	9.6 [m]
10.5 [b]	10.7± 0.03 [f]	23 [n]
11.8± 0.6 [c]	11.3± 0.03 [g]	11.6 [o]
12.1± 1 [d]	10.9± 0.04 [h]	20.4 [p]
	12 [i]	
	9.4 [j]	
	10.6 [k]	
	10.9 [l]	

[a] Reference 8.
[b] Reference 12.
[c] Reference 11.
[d] Reference 13.
[e] Reference 5.
[f] Reference 9, 300 °K.
[g] Reference 9, 77 °K.
[h] Reference 10, 200 °K.
[i] Reference 4.
[j] Reference 7.
[k] Reference 14.
[l] Reference 15.
[m] Reference 19.
[n] Reference 16.
[o] Reference 18.
[p] Reference 17.

These cells, with their diamond anvils used as windows, are especially suited to perform transmission measurements. At these high pressures, nonlinearity in the dependence of the energy of the E_0 gap on pressure might be expected.

Recent work shows that electron-phonon deformation potentials are extremely nonlinear as functions of the phonon coordinates.[22] This raises the question of how linear are the stress or strain deformation potentials of energy gaps. In order to elucidate this question for the hydrostatic deformation potentials we have measured the E_0 edge of GaAs by transmission through a thin sample in a diamond anvil cell. The pressure seemed to be nearly hydrostatic all the way up to 179 kbar, at which pressure a phase transition occurred. The dependence of the E_0 gap on pressure was shown to be substantially sublinear. The corresponding dependence on lattice constant a as a more fundamental quantity for the purpose of comparison with theoretical calculations, was still sublinear but only slightly so. In order to interpret these results we have performed pseudopotential calculations of the dependence of E_0 on a for GaAs using a Heine-Abarenkov pseudopotential with various assumptions about the dependence of the radius R of the region of zero potential on a. For R independent of a, a good fit to the linear portion of the dependence of E_0 on a was obtained, but, contrary to experiment, the calculated dependence was slightly superlinear. This discrepancy could only be remedied by introducing a somewhat artificial "hard core" term in the dependence of R on a. Calculations based on the empirical dielectric theory[19] yielded a poorer fit for the linear part of $E_0(a)$ but showed, at high pressures, a sublinearity in qualitative agreement with experiment.

II. EXPERIMENTAL METHOD

The inner portion of our diamond high-pressure cell is illustrated in Fig. 1. The two diamond anvils, of approximately $\frac{1}{6}$ carat each, are conventional brilliant cut gems with their culets polished down to form octagonal faces of about 0.8 mm across. They are cemented into small recesses in a pair of supporting pistons constructed of Vega tool steel, which had been hardened to Rockwell 63. The pistons slide smoothly within a retaining cylinder not shown. Provision is made to achieve coaxial alignment and parallelism of the culet faces by following the detailed design of Barnett *et al.*[21]

The working space of the cell is the cylindrical region bounded on top and bottom by the diamond and laterally by the wall of the steel gasket. The latter is made out of Waspalloy, annealed at a

temperature of 1200 °C in a hydrogen atmosphere. In practice the gasket material was precompressed by applying the necessary force with the diamonds, previously aligned interferometrically to better than one fringe, to reduce the thickness from 0.15 to 0.007 in. A 200-μm diam hole was then drilled in the center of the octagonal recess so formed and the gasket repositioned on the lower diamond.

The GaAs sample, which was electropolished from a (111) slab of carrier concentration $N = 10^{16}$ cm^{-3} to a thickness of 10 μm and broken into sufficiently small pieces, was inserted into the hole, resting flat on the lower diamond, together with several ruby chips needed for the measurement of the pressure. A few drops of a 4:1 mixture of methanol and ethanol were finally added as a pressure transmitting fluid and the second diamond quickly assembled within the apparatus with minimal pressure applied to form a seal.

Special problems are encountered in doing optical absorption in small samples. Since the beam must inevitably pass through four diamond surfaces, and also through a liquid medium whose refractive index is a function of pressure, accurate data can be obtained only by making a direct comparison of two measurements, one being the transmission through the sample proper and the other the transmission through a clear area beside the sample. The size of the beam must perforce be smaller than that of the sample since there is no possible way to mask the latter. One is therefore forced to employ a well-defined beam of diameter 30–50 μm. Furthermore, the fact that we wish to make transmission ratios as low as 10^{-4} places stringent requirements on the source brightness and the faithful imaging of that source within the cell.

A Xe 75-W high-pressure lamp was found to be the brightest source available at the wavelengths of interest. Its spectral distribution has sharp peaks in the region 0.8–1.0 μm, but for most of our measurements this is no impediment. The method of imaging this source within the cell is shown in Fig. 2. For this experiment we used a 30 μm aperture which was illuminated by focussing the lamp upon it with a 15× microscope objective. The aperture was located just behind a $\frac{1}{4}$-in. hole in the plane diagonal mirror and formed the effective source for the optical system which followed it. The cone of radiation leaving the aperture was incident upon a 6-in.-diam spherical mirror about 12 in. away, which was located accurately on the cone axis, and gave nearly 1:1 magnification. The mirror was furnished with micrometer adjustments to permit 3 deg of freedom in positioning the beam and focussing it sharply within the cell. With accurate alignment to assure precise on-axis operation the image of the circular aperture formed within the cell was very sharp and possessed minimal coma and no chromatic aberration. With this arrangement we estimate that the total radiation entering the cell was less than 2 mW. Since the sample was in fairly good thermal contact with the diamond faces via the alcohol, heating effects were entirely negligible (the gap obtained at atmospheric pressure agreed with that of Ref. 3 at room temperature).

The radiation leaving the cell through the upper

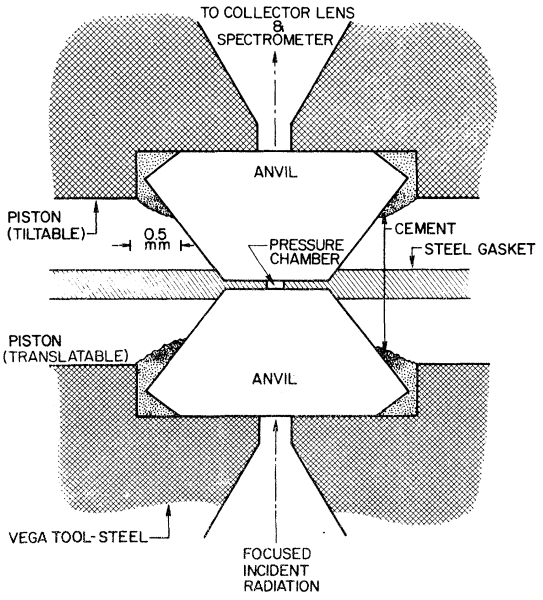

FIG. 1. Diagram of the diamond anvils and the pressure chamber used in our experiments.

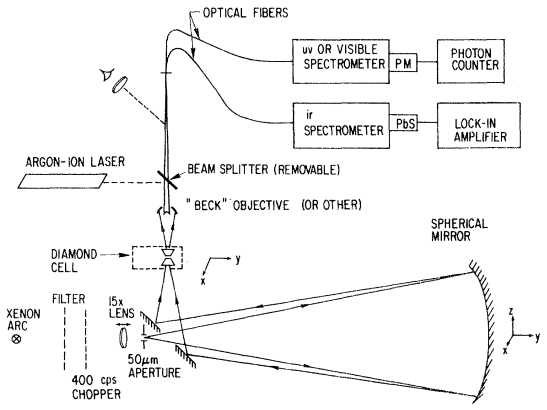

FIG. 2. Scheme of the setup used for the transmission measurements (Xenon Arc) and for the pressure measurements with the ruby manometer excited by the argon-ion laser.

diamond was collected by a reflecting type 15× microscope objective forming part of a standard microscope assembly. At the focal plane of the objective a bundle of optical fibers (suitably apertured to block any scattered light escaping around the sample) served as the conduit for the radiation. The fiber bundle terminated directly at the entrance slit of the monochromator, a Jarrel-Ash $\frac{1}{2}$-m grating instrument, where it was flared out in a vertical direction to match the slit width and height. The detector used was a cooled RCA 31034 photomultiplier especially suitable for low-level photon counting. The output from the photomultiplier was fed to a photon counting system (preamplifier-discriminator-ratemeter) and thence to a chart recorder.

To measure the pressure it proved very convenient to make use of the ruby fluorescence technique. It has been shown[21] that the wavelength of the R line doublet shifts extremely linearly with pressure at the rate $d\lambda/dP = -0.362$ Å/kbar. This relation is obtained from a direct comparison of the R line shift with the pressure shift in the lattice parameter of NaCl. Pressures are calculated using the Decker equation of state[23] for NaCl, and are estimated to be accurate to ±2%.

We believe that the pressure within our cell is very nearly hydrostatic throughout the range of our measurements. The uniformity of the pressure within the cell is easily verified by measuring the R line in different locations from several different chips scattered around the cell; no significant gradient could be detected even at the highest pressures. Furthermore, there was no evidence of broadening of the R line at any time.

Excitation of the R line is readily achieved with a few mW of power from the 5145-Å line of an Ar^+ laser. The radiation was introduced by inserting a beam splitter on the axis of the microscope tube. A normal microscope objective of glass was substituted in place of the reflecting objective, and a Corning 2-64 filter was located above the beam splitter to block the primary radiation. No detectable R line shift was observed when excitation power was increased by an order of magnitude. All measurements were performed at room temperatures.

III. RESULTS

The data obtained for several pressures up to 68 kbar are shown in Fig. 3. Figures 4 and 5 continue these data to higher pressures, using a smaller sample and hole. The data were taken over a period of several days, and the pressures were found to be remarkably stable. Moreover, some data were obtained after reducing the pressure, with no evidence of hysteresis.

In GaAs the E_0 absorption edge is strongly steepened by exciton formation; this effect makes itself felt even at 300 °K.[3] The "exciton" edge was located for each pressure by finding the energy at which the rising absorption coefficient sharply bends and becomes flat or as the intersection of the linearly extrapolated steep part with the flat part. This energy is found quite easily and accurately on the original chart recordings, and is less arbitrary than may appear in Figs. 3–5. We plot in Figs. 3–5 the ratio I_0/I vs $\hbar\omega$ on a logarithmic scale where I_0 is the intensity of the beam as it is transmitted alongside the sample, and I the transmitted intensity through the sample. Since our samples were 10 μm thick, $I_0/I \cong 10^3$ corresponds to $\alpha \simeq 7\times10^3$ cm^{-1}. In principle, the trans-

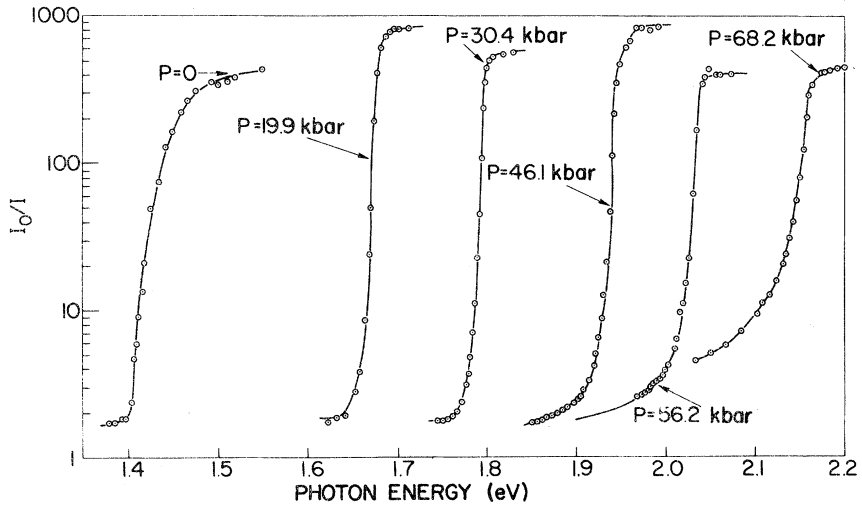

FIG. 3. Absorption edges of GaAs (I_0/I) for several pressures up to 68 kbar.

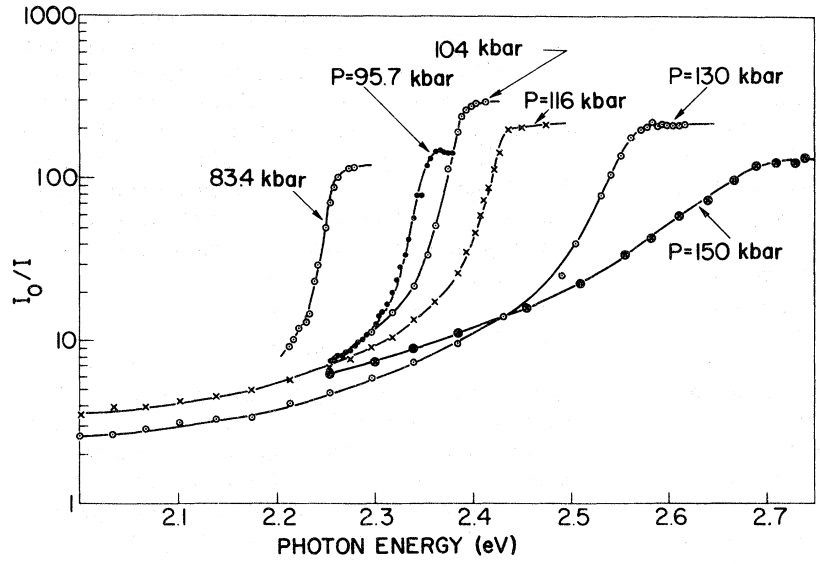

FIG. 4. Absorption edges of GaAs (I_0/I) for pressures between 83 and 150 kbar.

mission in the zero absorption region should increase steadily from 0.64 at $P=0$ to about 0.74 at $P=180$ kbar simply because of the increase in the refraction index of the alcohol mixture which improves optical matching to the sample. (The increase in the refractive index of the fluid can be estimated by means of the Clausius-Mosotti equation using the known density of methanol versus pressure.) We have made no attempt to compensate for this effect because the measured value of I_0 is in any case probably uncertain to (10–20)% due to the large filling factor and the progressive deformation of the hole in the gasket; under these conditions no reflection correction was made.

There is a low-energy tail which develops from about 40 kbar onwards, becoming more pronounced at the higher pressures. This represents the onset of the Γ-X indirect transition. According to Paul's rule the pressure coefficient of the Γ-X edge of GaAs should decrease with increasing pressure at a rate $dE/dp \simeq -1\times10^{-6}$ eV/bar. At $P=0$ the Γ-X transition lies about 0.36 eV above the E_0 edge[24]; as a consequence of the upward shift of E_0 the Γ-X indirect transition will drop below E_0 at about 35 kbar which is in conformity with the appearance of the tail between 30 and 46 kbar.

The shift of the E_0 edge versus pressure plotted for GaAs in Fig. 6 exhibits a pronounced nonlinear-

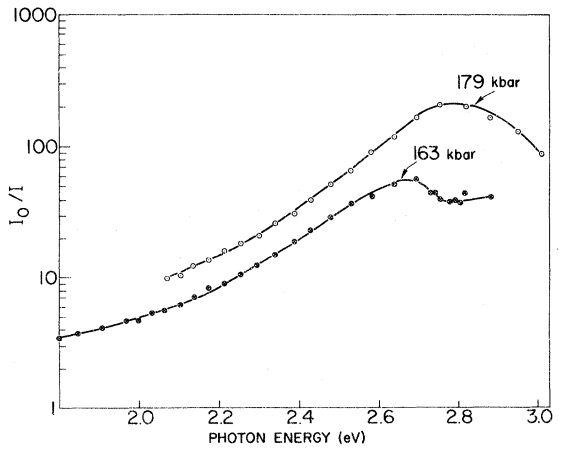

FIG. 5. Absorption edges of GaAs (I_0/I) for 163 and 179 kbar.

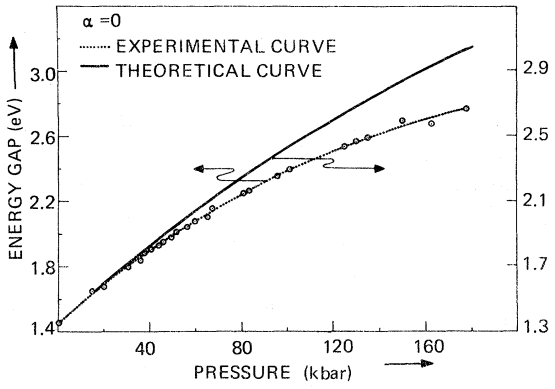

FIG. 6. E_0 edge of GaAs as a function of pressure. In this figure a theoretical curve is shown obtained in a manner described in Sec. IV. The parameter $\alpha=0$ indicates that the core radii used in Sec. IV are regarded as constants. Note further that the experimental and theoretical curves are displaced so that at $P=0$ they coincide. This remark applies also to Figs. 7–10. The experimental curve is a least squares fit with the polynomial $E_0(\text{eV}) = 1.45 + 1.26\times10^{-2}P - 3.77\times10^{-5}P^2$ (P in kbar). The standard deviation of this fit is 0.02 eV.

ity. Part of this nonlinearity is a consequence of the nonlinearity of the change of lattice parameter with pressure as will be shown in Sec. IV.

IV. THEORY AND DISCUSSION

In this section we describe the method used to calculate the pressure dependence of the direct energy gap (E_0) of GaAs. The energy levels of the crystal are functions of the lattice parameters, these functions being, in principle, obtained from the solution of the appropriate Schrödinger or Hartree-Fock equation for the valence and conduction electrons. In order to relate the calculations to the experimental results it is necessary to establish the connection between the volume of the crystal (i.e., of the lattice parameter) and the pressure. Unfortunately, there appears to be insufficient data on the equation of state of GaAs so that we are compelled to use one of two semiempirical universal equations of state which have been proposed. In the present work we use Murnaghan's equation.[25] This is equivalent to the assumption that the isothermal bulk modulus B is a linear function of the pressure P, i.e., that $B = B_0 + PB_0'$. The quantities B_0 and B_0' are, respectively, the bulk modulus and the derivative of the bulk modulus with respect to pressure, both at zero pressure. This assumption leads to the equation of state

$$P = (B_0/B_0')[(\Omega_0/\Omega)^{B_0'} - 1] , \quad (1)$$

where Ω_0 and Ω are the volumes at zero pressure and at pressure P, respectively.

Another semiempirical equation of state which is often used was given by Birch.[26] However, the latter gives results which do not differ significantly from those of Eq. (1) within the range of pressures of present interest. It is generally believed that Eq. (1) gives results of sufficient accuracy for our purposes. We use[27] $B_0 = 0.747 \times 10^{12}$ dyn/cm^2 and $B_0' = 4.67$.

The calculation of E_0 as a function of the lattice constant a is carried out supposing that the effective or pseudopotential, arising from the crystal potential and the effect of the orthogonalization of the plane wave states describing valence and conduction electrons to the core states, is small. We start with an empty fcc lattice and describe the "wave functions" of the valence electrons by

$$\langle \vec{r} | \vec{k} + \vec{K} \rangle = \Omega^{-1/2} \exp[i(\vec{k} + \vec{K}) \cdot \vec{r}] , \quad (2)$$

where $\vec{k}$ is the reduced wave vector and $\vec{K}$ a vector of the reciprocal lattice. For the fcc structure, the components of $\vec{K}$ along the cubic axes are $(2\pi/a) h_i$ $(i = 1, 2, 3)$. The numbers h_1, h_2, h_3 are integers, all of which have the same parity. We adopt the convention of taking the origin at the midpoint of a line joining a Ga atom to one of its nearest-neighbor As atoms. We take this vector to be $\vec{\rho} = (a/4)(1, 1, 1)$ so that there is a Ga atom at position $\frac{1}{2}\vec{\rho}$ and an As atom at $-\frac{1}{2}\vec{\rho}$. The empty lattice states at $\vec{k} = 0$ are labeled by the corresponding $\vec{K}$ vector and will be denoted by $(h_1 h_2 h_3)$. The first 15 states are (000), of energy zero, the eight states (111), $(\bar{1}11)$, $(1\bar{1}1)$, $(11\bar{1})$, $(\bar{1}\bar{1}1)$, $(\bar{1}1\bar{1})$, $(1\bar{1}\bar{1})$, $(\bar{1}\bar{1}\bar{1})$ (which we denote collectively by $\{111\}$) with energy $\frac{3}{2}(2\pi/a)^2$, and the six states (200), $(\bar{2}00)$, (020), $(0\bar{2}0)$, (002), and $(00\bar{2})$ with energy $2(2\pi/a)^2$. Here, and in what follows (unless otherwise noted), a and the energies are expressed in atomic units. The point group of the crystal is T_d so that the potential will, in general, split the degeneracies of the $\{111\}$ and $\{200\}$ levels. The eight $\{111\}$ states generate the reducible representation $2\Gamma_1 + 2\Gamma_{15}$ of T_d so that the corresponding levels split (we disregard here the effect of the electron spin) into two singlets and two triplets. In Table II, we give the reduction of the representations generated by (111) and (200) and their partners. The states f_1 and $f_2 = f_1^*$ are linearly independent and belong to Γ_1. The states of the set $\{111\}$ belonging to Γ_{15} are the sets X, Y, Z given in this Table and their complex conjugates. A similar notation is given for the decomposition of the subspace generated by (200) and its partners. The state (000) is designated by ϕ_0 and, of course, belongs to Γ_1.

We designate by A and B the two atoms of the lattice and by $\vec{n}$ a vector of the lattice. Then, we write the pseudopotential as

$$V(\vec{r}) = \sum_n [v_A(\vec{r} - \vec{n} - \tfrac{1}{2}\vec{\rho}) + v_B(\vec{r} - \vec{n} + \tfrac{1}{2}\vec{\rho})] , \quad (3)$$

where v_A and v_B are the contributions of the atoms A and B to the crystal pseudopotential, respectively.

The matrix element of $V(\vec{r})$ between the states $|\vec{k} + \vec{K}\rangle$ and $|\vec{k} + \vec{K}'\rangle$ is

$$\langle \vec{k} + \vec{K} | V(\vec{r}) | \vec{k} + \vec{K}' \rangle$$

$$= v_{\vec{K}, \vec{K}'}$$

$$= v^{(s)}(\vec{G}) \cos\left(\frac{\vec{G} \cdot \vec{\rho}}{2}\right) + i v^{(a)}(\vec{G}) \sin\left(\frac{\vec{G} \cdot \vec{\rho}}{2}\right), \quad (4)$$

where

$$\vec{G} = \vec{K} - \vec{K}' , \quad (5)$$

$$v^{(s,a)}(\vec{G}) = \tfrac{1}{2}[v_A(\vec{G}) \pm v_B(\vec{G})] , \quad (6)$$

$$v_A(\vec{G}) = \frac{2}{\Omega} \int e^{i\vec{G} \cdot \vec{r}} v_A(\vec{r})\, d\vec{r} , \quad (7)$$

and a similar expression for $v_B(\vec{G})$. Here Ω is the volume of the primitive cell, i.e., twice the volume

TABLE II. Reduction of the representations generated by (000), (111), and (200), and their partners.

(i) $\Gamma(000)=\Gamma_1$, $\phi_0=(000)$,

(ii) $\Gamma(111)=2\Gamma_1+2\Gamma_{15}$,

Γ_1: $f_1=\frac{1}{2}[(111)-(1\bar{1}\bar{1})-(\bar{1}1\bar{1})-(\bar{1}\bar{1}1)]$,

$f_2=\frac{1}{2}[(\bar{1}\bar{1}\bar{1})-(\bar{1}11)-(1\bar{1}1)-(11\bar{1})]=f_1^*$,

Γ_{15}: $X=\frac{1}{2}[(111)-(1\bar{1}\bar{1})+(\bar{1}1\bar{1})+(\bar{1}\bar{1}1)]$,

$Y=\frac{1}{2}[(111)+(1\bar{1}\bar{1})-(\bar{1}1\bar{1})+(\bar{1}\bar{1}1)]$,

$Z=\frac{1}{2}[(111)+(1\bar{1}\bar{1})+(\bar{1}1\bar{1})-(\bar{1}\bar{1}1)]$,

$X'=X^*$,
$Y'=Y^*$,
$Z'=Z^*$.

(iii) $\Gamma(200)=\Gamma_1+\Gamma_{12}+\Gamma_{15}$

Γ_1: $\phi=(1/\sqrt{6})[(200)+(020)+(002)-(\bar{2}00)-(0\bar{2}0)-(00\bar{2})]$.

Γ_{15}: $\xi=(1/\sqrt{2})[(200)+(\bar{2}00)]$,

$\eta=(1/\sqrt{2})[(020)+(0\bar{2}0)]$,

$\zeta=(1/\sqrt{2})[(002)+(00\bar{2})]$.

Γ_{12}: $g_1=\frac{1}{2}[(200)-(\bar{2}00)-(020)+(0\bar{2}0)]$,

$g_2=[1/(12)^{1/2}][(200)-(\bar{2}00)+(020)-(0\bar{2}0)-2(002)+2(00\bar{2})]$.

per atom.

In Table III we give the matrix elements of the pseudo-Hamiltonian $H=-\frac{1}{2}\nabla^2+V$ for the three Γ_{15} states X, X', and ξ. The quantities T_0 and $v_\nu^{(s,a)}$ are defined in Table III. Table IV displays the matrix elements of H for the states $\phi_0 f_1$, f_2 and ϕ which belongs to Γ_1.

For the purpose of the numerical calculation we follow Cohen and Heine[28] and use the expression

$$v(q)=-\frac{8\pi z}{q^2\epsilon(q)}\frac{\cos(qR)}{\Omega} \tag{8}$$

for $v_{A,B}(q)$ in Eq. (7). Here $v(q)$ is in atomic units and z is the number of outer electrons per atom ($z=3$ for Ga, and $z=5$ for As); R is an atomic core radius.[29] The screening of the core potential by the electrons is taken into account using the dielectric function[30]

$$\epsilon(q)=1-\frac{16\pi}{\Omega q^2}\left(1-\frac{q^2/2}{q^2+k_F^2+k_s^2}\right)\chi(q)\,, \tag{9}$$

with

$$\chi(q)=-\frac{z}{2}\left(\frac{2}{3}E_{F0}\right)^{-1}\left(\frac{1}{2}+\frac{4k_F^2-q^2}{8qk_F}\ln\left|\frac{2k_F+q}{2k_F-q}\right|\right), \tag{10}$$

where z is the number of outer electrons per atom, $z=\frac{1}{2}(z_A+z_B)$, $E_{F0}=\frac{1}{2}k_F^2$ the free-electron bandwidth, and $k_s=(2k_F/\pi)^{1/2}$ a screening parameter. Note that the latter differs from the Thomas-Fermi screening parameter $(4k_F/\pi)^{1/2}$ by a factor of $2^{-1/2}$. The expressions for $v^{(s,a)}(q)$ are

$$v^{(s,a)}(q)=-[4\pi/q^2\epsilon(q)\Omega]\times[z_A\cos(qR_A)\pm z_B\cos(qR_B)]\,. \tag{11}$$

Since $v^{(s,a)}(q)$ depends on the magnitude of q alone

TABLE III. Matrix of $H=-\frac{1}{2}\nabla^2+V$ for the three Γ_{15} states X, X', ξ. Here $T_0=\frac{1}{2}(2\pi/a)^2$ and $v^{(a)}_{h_1^2+h_2^2+h_3^2}=v^{(a)}(\vec{G}_{h_1h_2h_3})$. A similar definition is given for $v^{(s)}_{h_1^2+h_2^2+h_3^2}$.

	X	X'	ξ
X	$3T_0-v_8^{(s)}$	$-iv_4^{(a)}+iv_{12}^{(a)}$	$(v_3^{(s)}-iv_3^{(a)})-(v_{11}^{(s)}-iv_{11}^{(a)})$
X'	$iv_4^{(a)}-iv_{12}^{(a)}$	$3T_0-v_8^{(s)}$	$(v_3^{(s)}+iv_3^{(a)})-(v_{11}^{(s)}+iv_{11}^{(a)})$
ξ	$(v_3^{(s)}+iv_3^{(a)})-(v_{11}^{(s)}+iv_{11}^{(a)})$	$(v_3^{(s)}-iv_3^{(a)})-(v_{11}^{(s)}-iv_{11}^{(a)})$	$4T_0-v_{16}^{(s)}$

TABLE IV. Matrix of H for the four Γ_1 states ϕ_0, f_1, f_2, ϕ.

	ϕ_0	f_1	f_2	ϕ
ϕ_0	0	$-\sqrt{2}(v_3^{(s)}-iv_3^{(a)})$	$-\sqrt{2}(v_3^{(s)}+iv_3^{(a)})$	$i\sqrt{6}v_4^{(a)}$
f_1	$-\sqrt{2}(v_3^{(s)}+iv_3^{(a)})$	$3T_0+3v_8^{(s)}$	$3iv_4^{(a)}+iv_{12}^{(a)}$	$\sqrt{3}(v_3^{(s)}-iv_3^{(a)})+\sqrt{3}(v_{11}^{(s)}-iv_{11}^{(a)})$
f_2	$-\sqrt{2}(v_3^{(s)}-iv_3^{(a)})$	$-3iv_4^{(a)}-iv_{12}^{(a)}$	$3T_0+3v_8^{(s)}$	$-\sqrt{3}(v_3^{(s)}+iv_3^{(a)})-\sqrt{3}(v_{11}^{(s)}+iv_{11}^{(a)})$
ϕ	$-i\sqrt{6}v_4^{(a)}$	$\sqrt{3}(v_3^{(s)}+iv_3^{(a)})+\sqrt{3}(v_{11}^{(s)}+iv_{11}^{(a)})$	$-\sqrt{3}(v_3^{(s)}-iv_3^{(a)})-\sqrt{3}(v_{11}^{(s)}-iv_{11}^{(a)})$	$4T_0+4v_8^{(s)}+v_{16}^{(s)}$

and we require the values of these quantities for $|\vec{G}|=(2\pi/a)(h_1^2+h_2^2+h_3^3)^{1/2}$ it will be enough to label them by $\nu=h_1^2+h_2^2+h_3^2$. This has already been indicated in Tables III and IV. As is customary, we keep only the Fourier components of the pseudopotential with $\nu<11$.

The numerical calculations were done using the values of R_A, R_B given in Table XVIII of Ref. 28 which were adjusted to experimental data. It is convenient to define q_A and q_B such that $q_{A,B}R_{A,B}=(\pi/2)$. The values used in our calculations were $q_{Ga}=1.49$ and $q_{As}=1.65$. These cutoffs were adjusted[28] using pseudopotential calculations with more plane waves than we employed in the present work, so that our calculated zero pressure gap is not identical to the experimental one. The results are displayed in Fig. 7 where the experimental results of Fig. 6 have also been plotted after use has been made of Murnaghan's equation. In Fig. 6 we had also shown the theoretical results versus pressure. We note that, while there is substantial agreement in the linear variation of E_0 with $\Delta a/a_0$, the experimental curve is slightly sublinear while the theoretical one is superlinear.

It is natural to modify the calculation assuming that R_A and R_B change with the lattice parameter. In fact, one can readily convince oneself that as the lattice parameter decreases the core radius of a constituent atom should decrease. In Fig. 8 we plot E_0 vs $\Delta a/a_0$ supposing $R_{A,B}=R_{A,B}^{(0)}(1+\alpha\Delta a/a_0)$ for the value of $\alpha=0.23$. This leads again to a superlinear variation of E_0 with $\Delta a/a_0$. This difficulty can only be remedied by selecting quadratic variations of $R_{A,B}$ with $\Delta a/a_0$. The results of such a calculation of E_0 as a function of $\Delta a/a_0$ are shown in Fig. 9 and the corresponding variation with pressure is displayed in Fig. 10. In all these graphs the experimental curves have been drawn

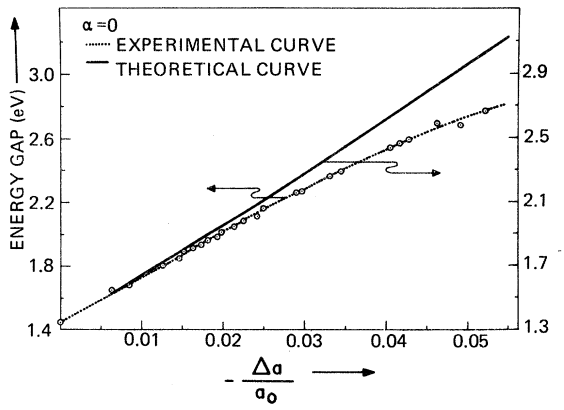

FIG. 7. E_0 edge of GaAs as a function of the lattice parameter a.

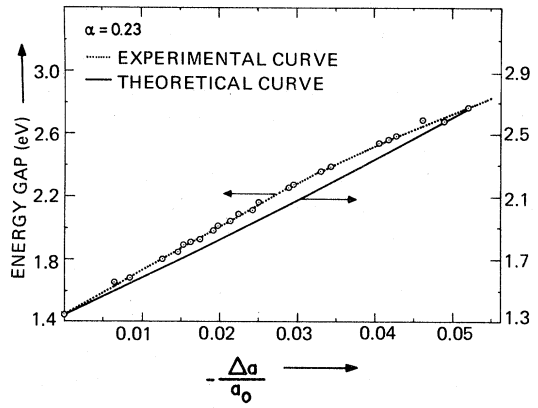

FIG. 8. E_0 edge of GaAs as a function of a. It was assumed that $R_{A,B} = R^{(0)}_{A,B}(1 + \alpha \Delta a/a_0)$ with $\alpha = 0.23$.

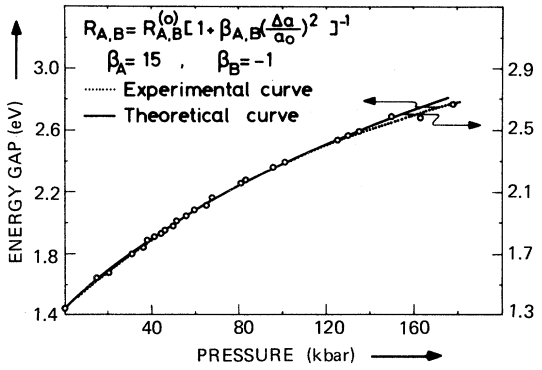

FIG. 10. Same as Fig. 9 but displayed as a function of pressure P.

to facilitate comparison with the theory. The variations of R_A and R_B (A = Ga, B = As) shown in Figs. 9 and 10 are consistent with a quadratic decrease in ionicity with increasing pressure. Such decrease is also suggested by recent experiments on the Raman effect in GaAs under hydrostatic pressure.[31]

Finally, a calculation of E_0 as a function of lattice parameter was made using the empirical dielectric theory of Van Vechten.[32,33] For this we used Eq. (3.7) of Ref. 33 with modifications introduced by Camphausen *et al.*[19] The results of the calculation are displayed in Fig. 11. We see that the agreement is qualitative but not quantitative. What is interesting about this result is that the calculated energy gap E_0 is sublinear as a function of $\Delta a/a_0$, in agreement with the experimental findings. This sublinearity is due to the strong effect of the d core electrons of the Ga on the Γ_1 conduction band.[33] We are thus left with two possible qualitative explanations of the sublinearity in the pressure dependence of E_0 in GaAs. One has to do with a quadratic decrease in the ionicity when compressing from the equilibrium lattice constant a_0 and the other with the metallization effect of the outermost d core electrons. An operational way of distinguishing between these two explanations is to measure Ge and Si, both nonionic and the latter without core d electrons. Preliminary measurements of the pressure dependence of the E_0 (gap $\Gamma_{25'} \rightarrow \Gamma_{2'}$) of[33] Ge yield a sublinear dependence of E_0 similar to that observed for GaAs thus ruling out any explanation based on a pressure dependence of the ionicity. For Si,[34] measurements of the $\Gamma_{25'} \rightarrow X_1$ *indirect* gap yield a linear dependence up to 100 kbar. Although this gap is less sensitive to d electrons than the $\Gamma_{25'} \rightarrow \Gamma_{2'}$ or E_0 gap, the linearity observed, which agrees with pseudopotential calculations, is consistent with the absence of d electrons in the case of the Si atoms.

Finally, if we write

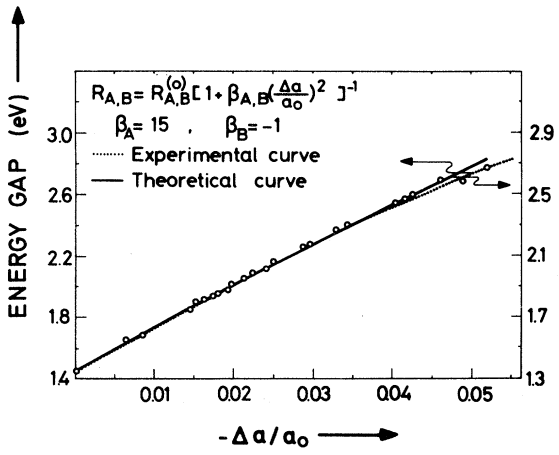

FIG. 9. E_0 edge of GaAs as a function of a, assuming that the core radii vary quadratically with $\Delta a = a - a_0$.

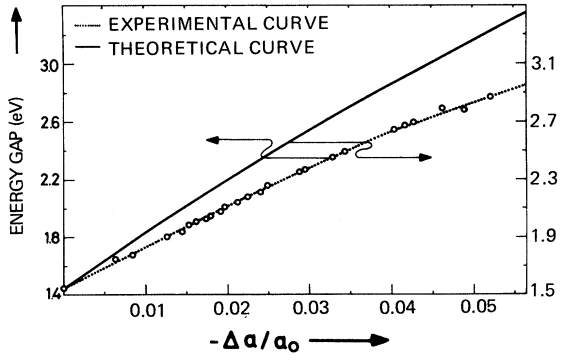

FIG. 11. Calculated value of the E_0 edge of GaAs using the empirical dielectric theory with the experimental results.

$$E_0(a) = E_0(a_0) + A\,\Delta a/a_0 + B(\Delta a/a_0)^2 + \cdots, \quad (12)$$

the best fit to the experimental results is given for $A = -29.3$ eV and $B = -57.5$ eV, i.e., the coefficients are of the same order of magnitude. This is in contrast with the large nonlinearity of the electron-phonon deformation potentials on the optical-phonon coordinates mentioned above.[22]

ACKNOWLEDGMENTS

We acknowledge helpful conversations with M. Brodsky, V. Heine, W. E. Howard, J. A. Van Vechten, and R. W. Keyes. Also, thanks are due to John Marinace for furnishing the material and valuable advice on samples preparation, and to W. Holzapfel, G. Piermarini, and B. A. Weinstein for their advice on high-pressure techniques.

*Permanent address.
† Supported in part by the NSF. On leave from Purdue University, West Lafayette, Ind. 47907
‡ Alexander von Humboldt Senior U. S. Scientist on sabbatical leave from Purdue University, West Lafayette, Ind. 47907.

[1]See, for instance, W. Paul, in *The Optical Properties of Solids*, edited by J. Tauc (Academic, New York, 1966), p. 257.
[2]W. Paul, J. Phys. Chem. Solids 8, 196 (1958).
[3]M. D. Sturge, Phys. Rev. 127, 768 (1962).
[4]D. M. Warschauer and W. Paul (unpublished).
[5]R. Bendorius and A. Shileika, Solid State Commun. 8, 1111 (1970).
[6]R. A. Fitch, T. E. Slykhouse, and H. G. Drickamer, J. Opt. Soc. Am. 47, 1015 (1957).
[7]A. L. Edwards, T. E. Slykhouse, and H. G. Drickamer, J. Phys. Chem. Solids 11, 140 (1959).
[8]F. H. Pollak and M. Cardona, Phys. Rev. 172, 816 (1968).
[9]J. Feinleib, S. Groves, W. Paul, and R. Zallen, Phys. Rev. 131, 2070 (1963).
[10]G. E. Fenner, J. Appl. Phys. 34, 2955 (1963).
[11]R. N. Bhargava and M. I. Nathan, Phys. Rev. 161, 695 (1967).
[12]I. Balslev, Solid State Commun. 5, 315 (1967).
[13]J. Wajda and M. Grynberg, Phys. Status. Solidi 37, K55 (1970).
[14]A. R. Hutson, A. Jayaraman, and A. S. Coriell, Phys. Rev. 155, 786 (1967).
[15]A. Jayaraman, M. E. Sikorski, J. C. Irvin, and G. H. Yates, J. Appl. Phys. 38, 4454 (1967).
[16]T. C. Collins, D. J. Stukel, and R. N. Euwema, Phys. Rev. B 1, 724 (1970).
[17]P. J. Melz, J. Phys. Chem. Solids 28, 144 (1967).
[18]H. Neumann, I. Topol, K. R. Schulze, and E. Hess, Phys. Status Solidi B 56, K55 (1973).
[19]D. L. Camphausen, G. A. N. Connell, and W. Paul, Phys. Rev. Lett. 26, 184 (1971).
[20]P. J. Melz and I. B. Ortenburger, Phys. Rev. B 3, 3257 (1971).
[21]J. D. Barnett, S. Block, and G. J. Piermarini, Rev. Sci. Instrum. 44, 1 (1973); G. J. Piermarini, S. Block, and J. D. Barnett, J. Appl. Phys. 44, 5377 (1973).
[22]P. J. Lin-Chung and K. Ngai, Phys. Rev. Lett. 29, 1610 (1972).
[23]D. L. Decker, J. Appl. Phys. 37, 5012 (1966).
[24]L. W. James and J. L. Moll, Phys. Rev. 183, 740 (1969).
[25]F. D. Murnaghan, Proc. Nat. Acad. Sci. 30, 244 (1944).
[26]F. Birch, Phys. Rev. 71, 809 (1947), J. Geophys. Res. 57, 227 (1952).
[27]H. J. McSkimin, A. Jayaraman, and P. Andreatch, J. Appl. Phys. 38, 2362 (1967).
[28]M. L. Cohen and V. Heine, *Solid State Physics*, edited by H. Ehrenreich, F. Seitz, and D. Turnbull (Academic, New York, 1970), Vol. 24, p. 37.
[29]The bare potential is of the form $-z/r$ for $r > R$ and zero for $r < R$.
[30]This is the dielectric function used by L. J. Sham, Proc. R. Soc. A 283, 33 (1965). See also Ref. 28, p. 52.
[31]R. Trommer and M. Cardona, Proceedings of the Third International Conference on Light Scattering in Solids, Campinas, Brazil, 1975 (to be published).
[32]J. A. Van Vechten, Phys. Rev. 182, 891 (1969).
[33]J. A. Van Vechten, Phys. Rev. 187, 1007 (1969).
[34]B. Welber, C. K. Kim, M. Cardona, and S. Rodriguez (unpublished).